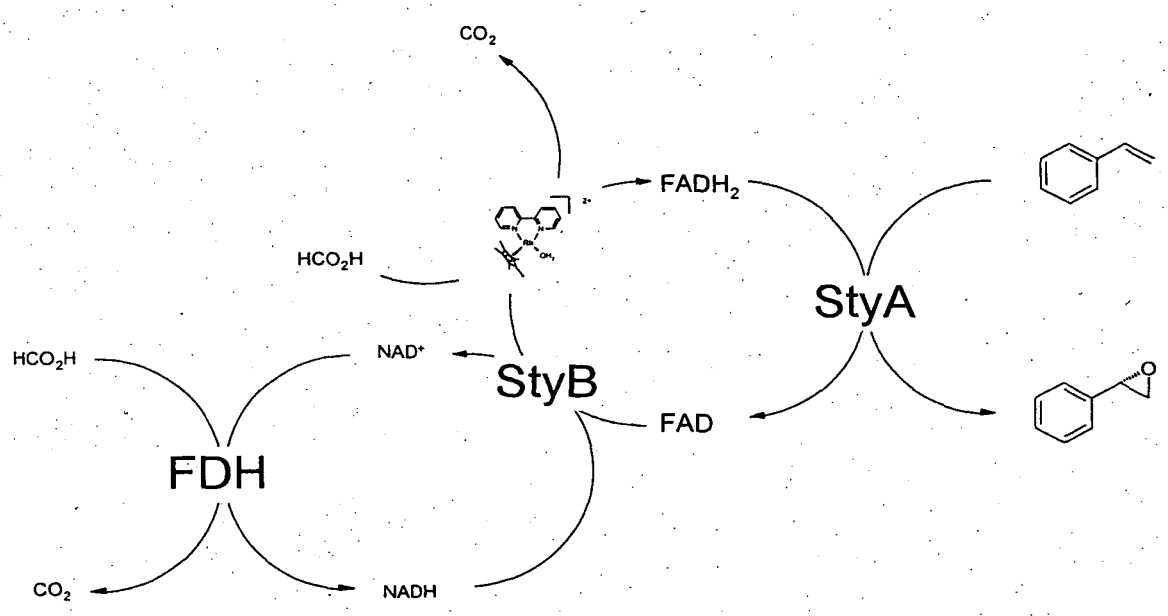

Figure 1: In vitro regeneration of styrene monooxygenase (StyA). $[Cp^*Rh(bpy)(H_2O)]^{2+}$ catalyzed regeneration (upper) compared to a reductase-catalyzed setup (e.g. utilizing the native reductase StyB) with NAD(P)H regeneration.

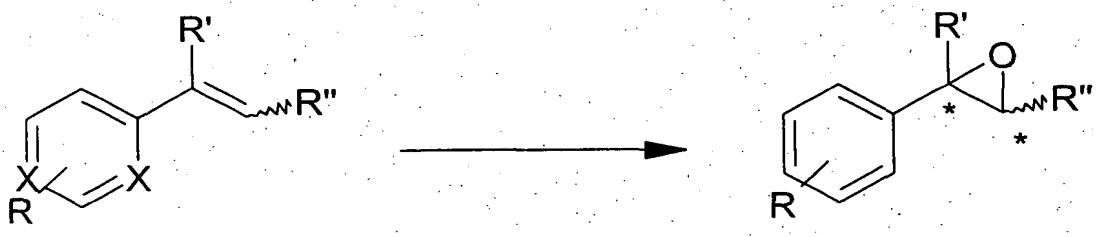

R = H, 3-methyl, 4-methyl, 4-F, 4-Cl, 4-Br,3-Br, 3-NO_2
R' = H, methyl
R" = H, *trans*-methyl
X = C, N

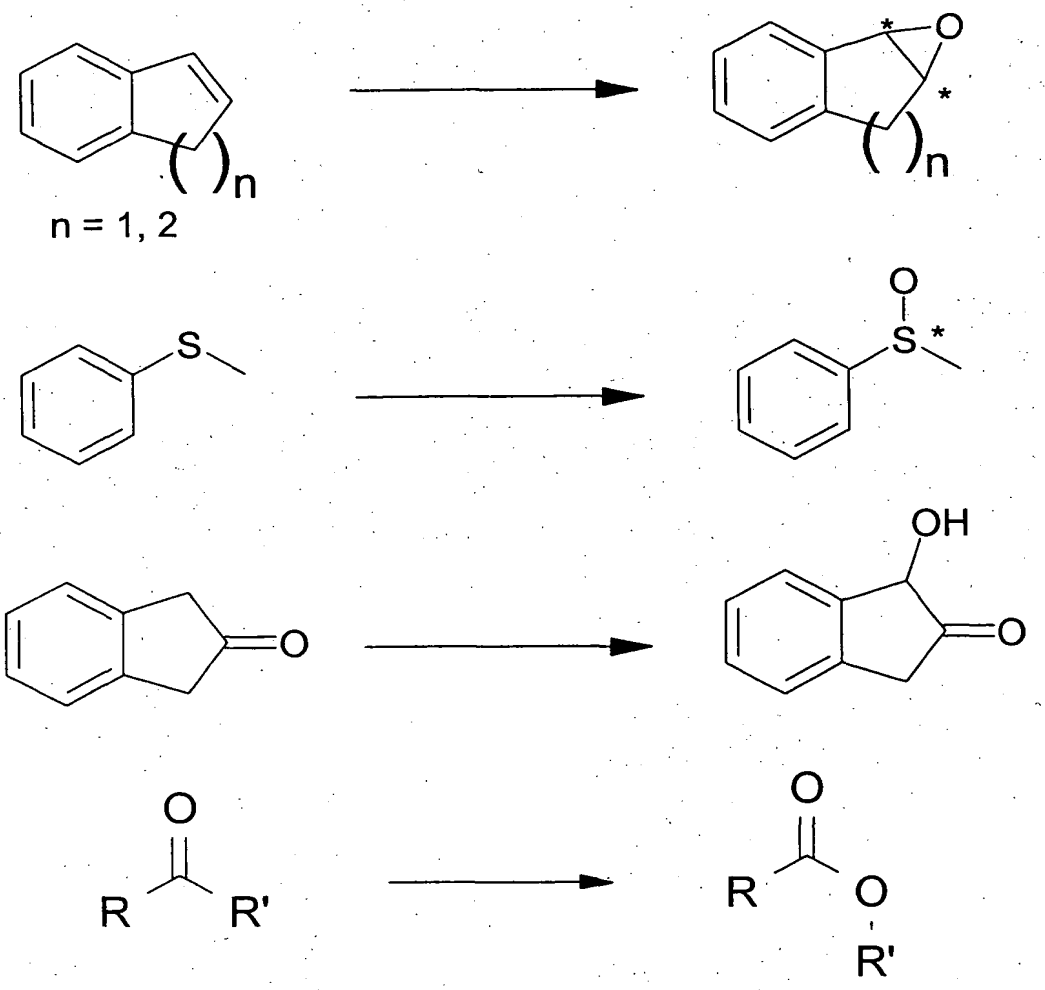

Figure 2: Examples for StyA-cataylyzed oxidation reactions.

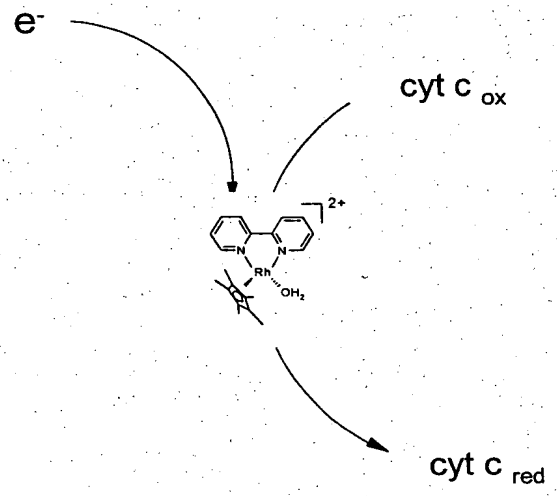

Figure 3: [Cp*Rh(bpy)H]$^+$ catalyzed and formate driven reduction of CytC. Electrons are derived either from chemical reductants (such as formate) or from the cathode.

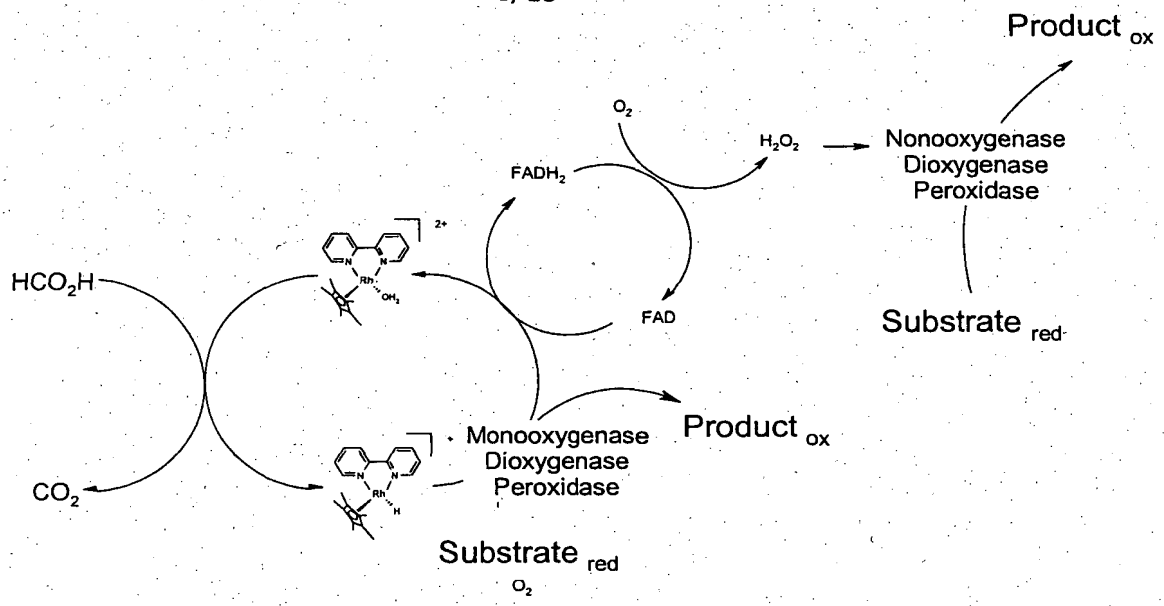

Figure 4: Summarized regeneration pathways of *in vitro* regeneration of monooxygenases and peroxidases.

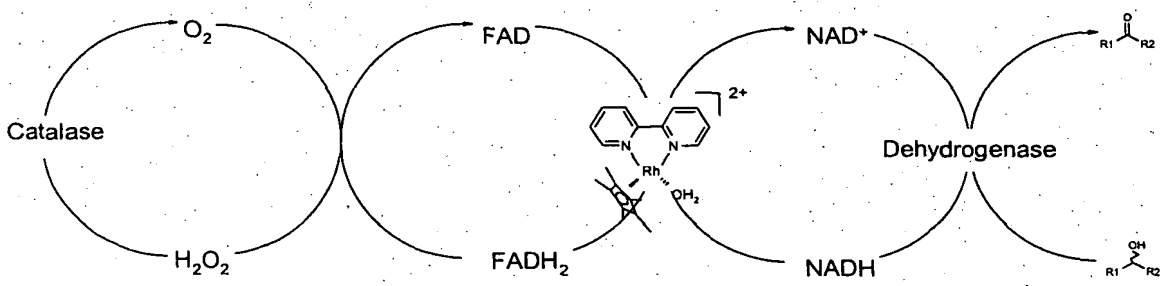

Figure 5: Transhydrogenation from NAD(P)H to FAD (FMN) catalyzed by $Cp^*Rh(bpy)(H_2O)]^{2+}$ and its application to dehydrogenase catalyzed oxidation reactions.

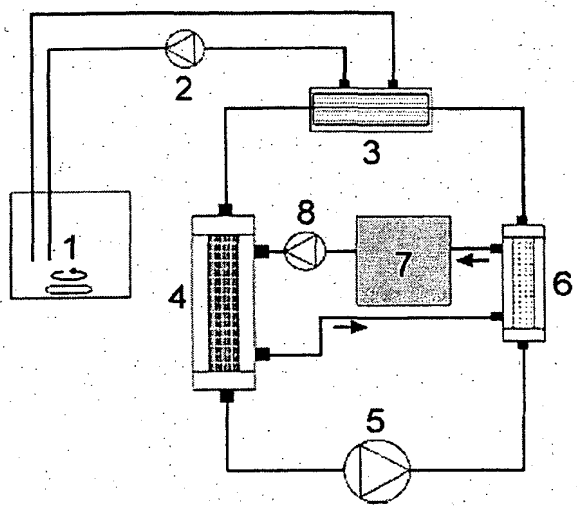

Figure 6: Schematic setup of a compartmented electrochemical setup with immobilized biocatalyst. (1) stirred reservoir for substrates and products in a suitable solvent; (2) pump; (3) hollow-fibre module; (4) flow-through electrolysis cell (connected to a potentiostat); (5) pump; (6) immobilized biocatalyst (7) thermostat (8) pump.

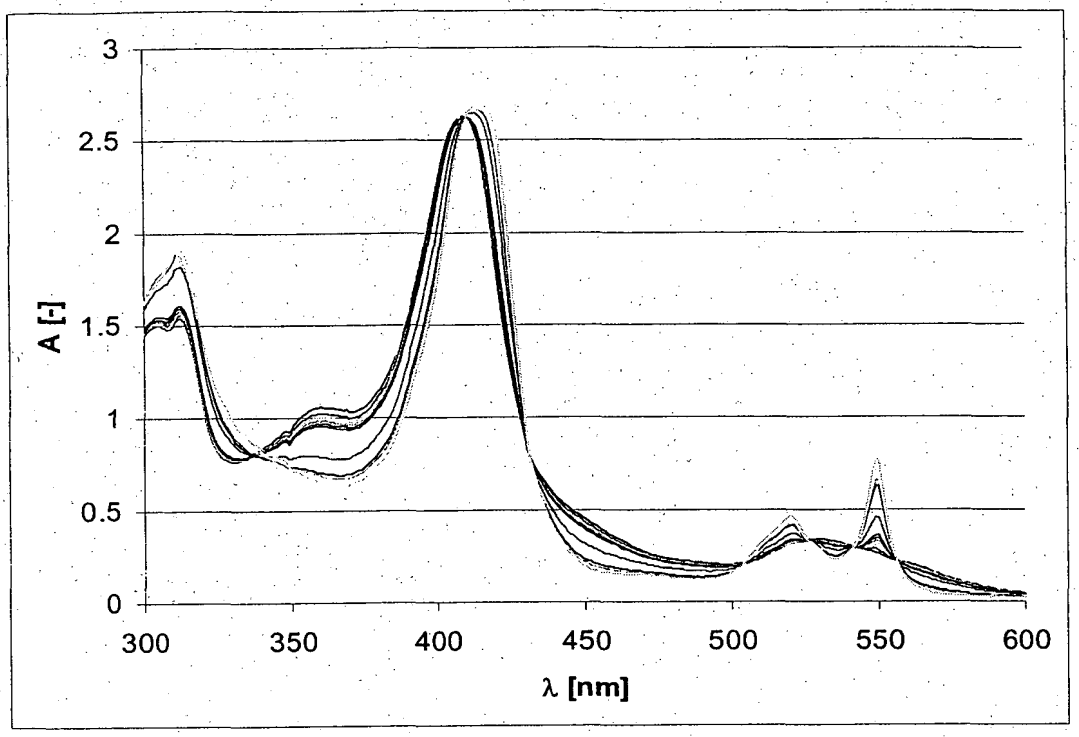

Figure 7: UV-spectra of CytC while incubation with hydrogen peroxide.

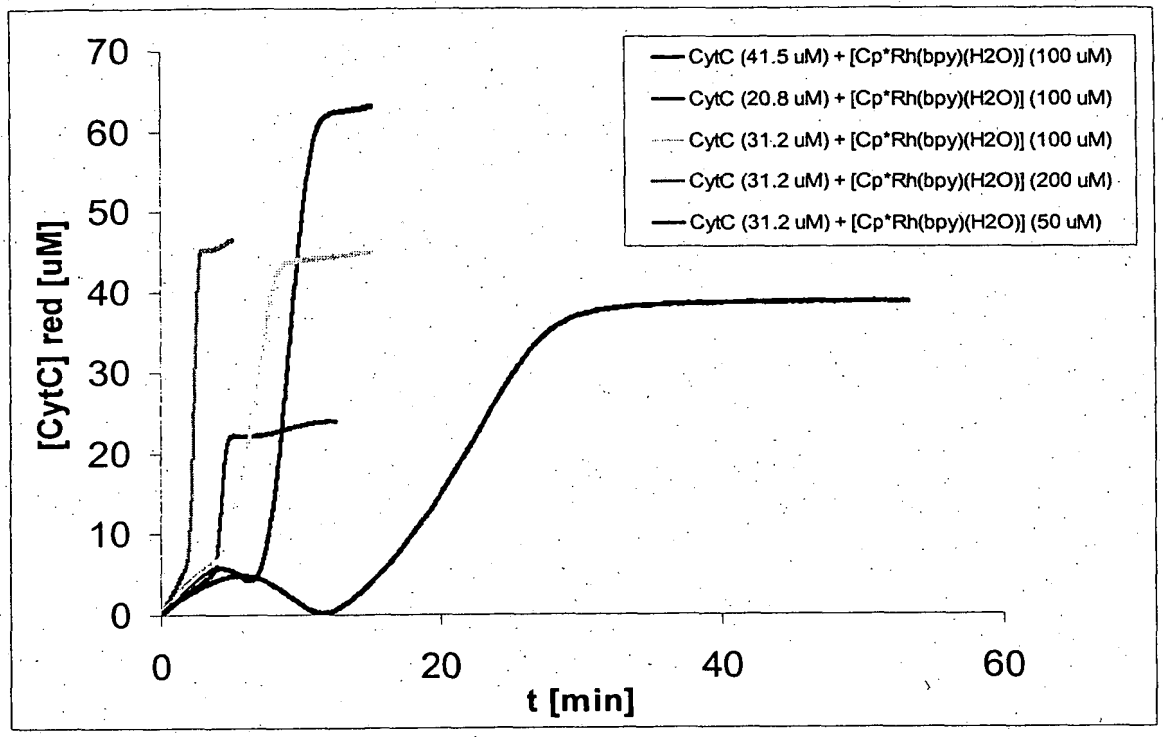

Figure 8: Experiments on varying c([Cp*Rh(bpy)(H_2O)]$^{2+}$) and c(CytC).

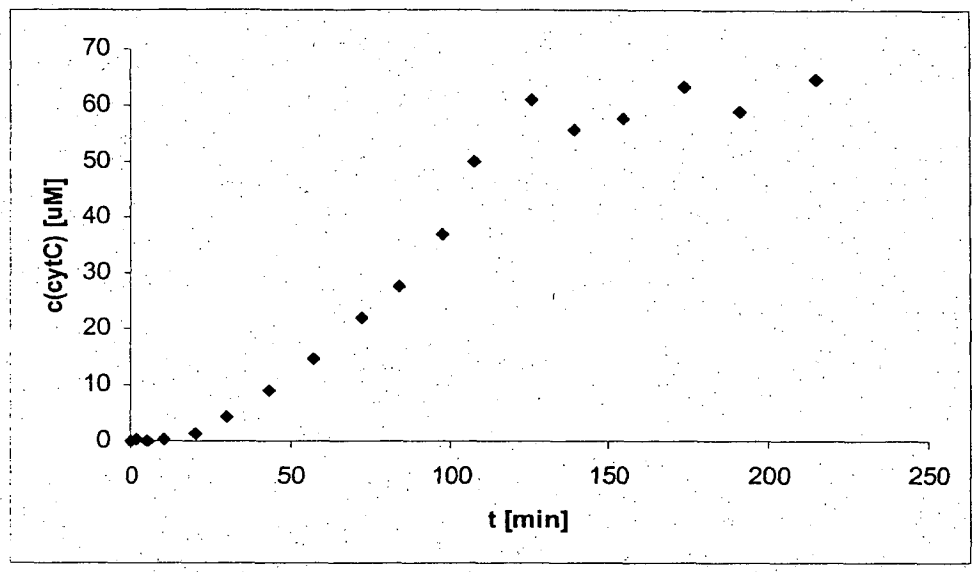

Figure 9: Sub-stochiometric use of $[Cp^*Rh(bpy)(H_2O)]^{2+}$. $c([Cp^*Rh(bpy)(H_2O)]^{2+})$ = 10 μM, c(cytC)= 80 μM, $c(NaHCO_2)$ = 150 mM, T= 30 °C, degassed buffer.

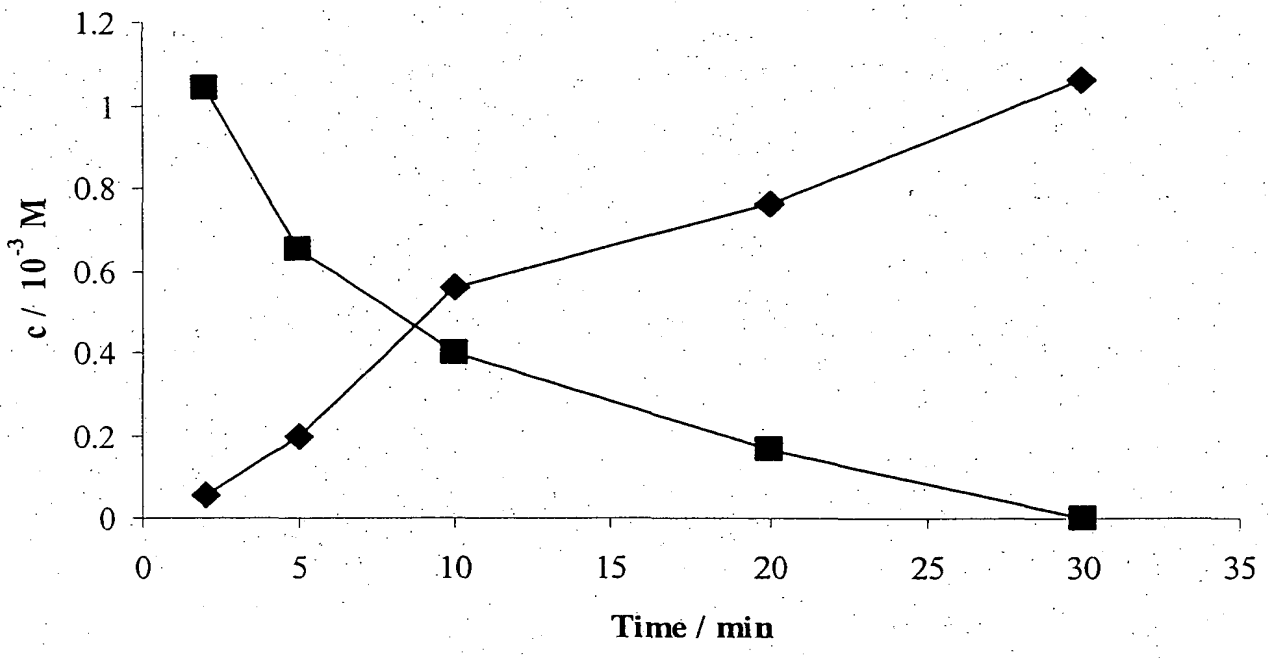

Figure 10: Time course of $[Cp^*Rh(bpy)(H_2O)]^{2+}$-driven and StyA-catalyzed epoxidation of styrene. Styrene oxide (—◆—); styrene (—■—). T = 37 °C; c($NaHCO_2$) = 0.15 M; c($[Cp^*Rh(bpy)(H_2O)]^{2+}$) = 2×10^{-4} M: c(FAD) = 5×10^{-5} M; c(FMN) = 5×10^{-6} M: catalase = 28 U × ml^{-1}; c_o (styrene) = 2×10^{-3} M; c(StyA) = 50 µg × ml^{-1} = 1.16×10^{-6} M

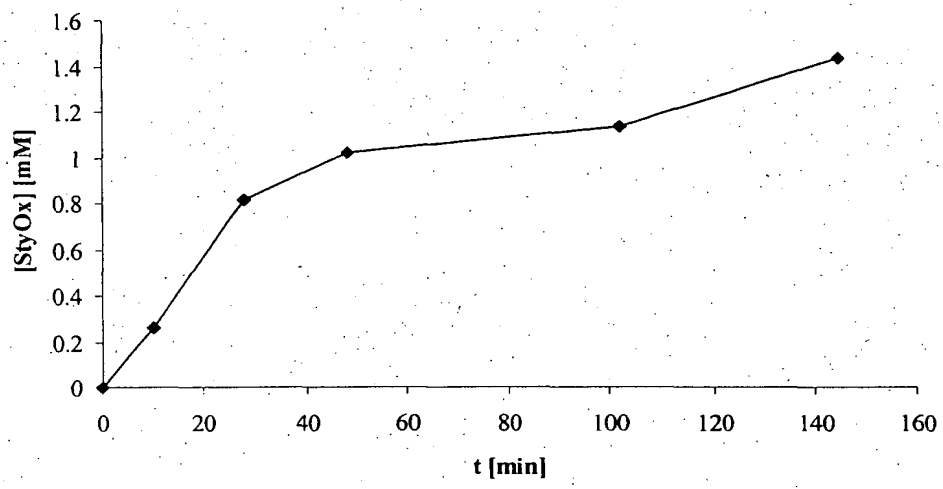

Figure 11: Styrene oxide formation in the presence of neat styrene as 2nd organic phase (substrate & product reservoir).

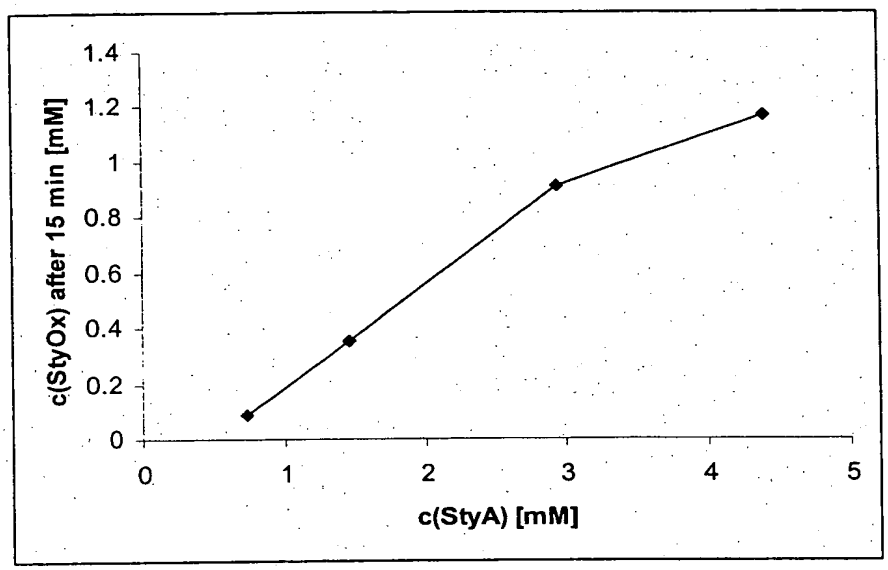

Figure 12: Styrene oxide concentration after 15 min incubation on variation of c(StyA).

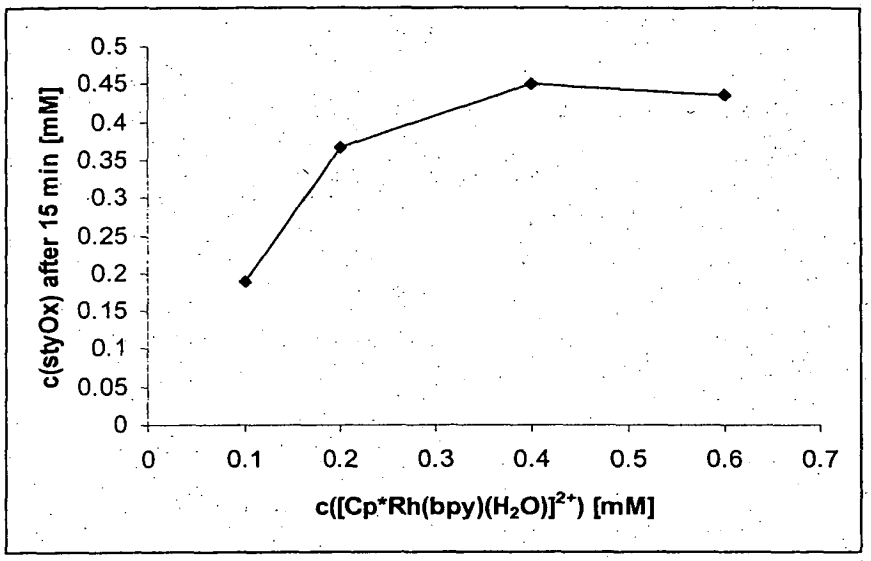

Figure 13: Styrene oxide concentration after 15 min incubation on variation of c($[Cp^*Rh(bpy)(H_2O)]^{2+}$).

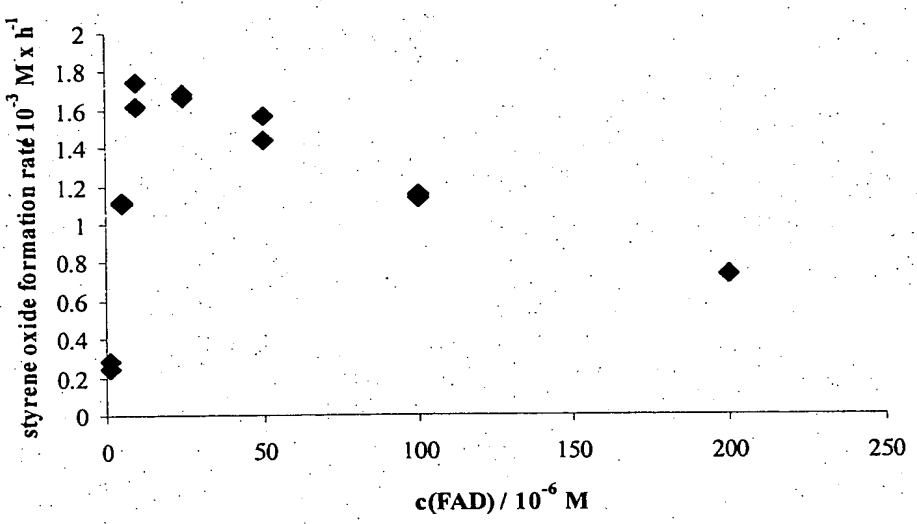

Figure 14: Styrene oxide formation rate as a function of c(FAD). c([Cp*Rh(bpy)(H_2O)]$^{2+}$) = 0.2 mM; c(StyA) = 1.25 µM; Catalase 280 U; c(styrene) = 2 mM; T = 37 °C.

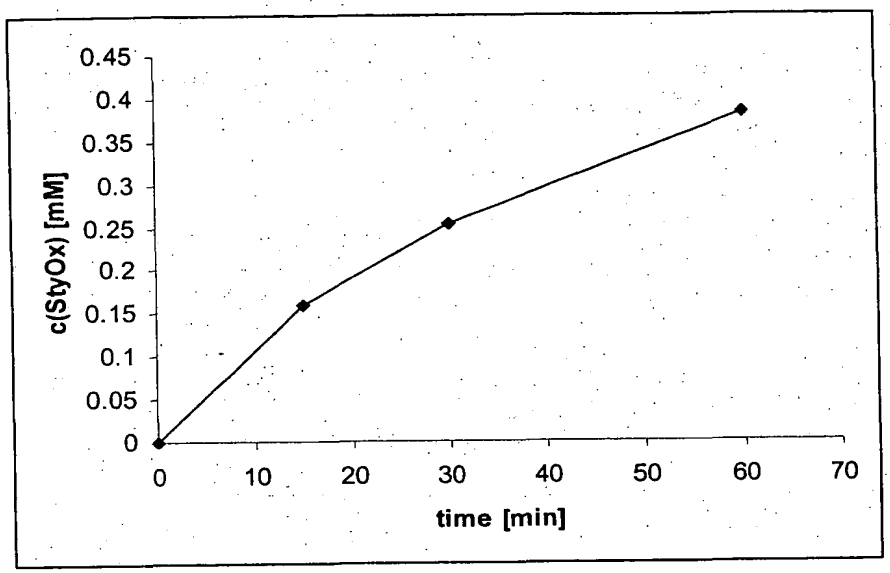

Figure 15: Styrene oxide (StyOx) formation using immobilized StyA.

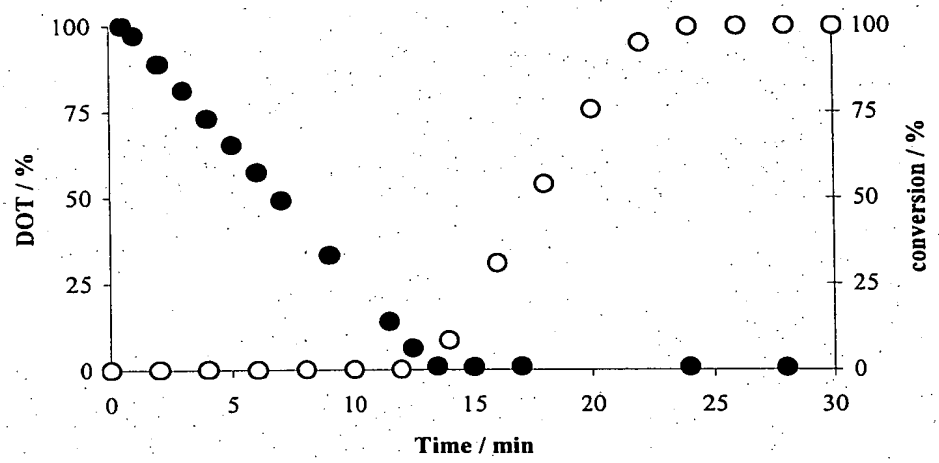

Figure 16: Time course of dissolved oxygen (DOT) (●) and c($FADH_2$) (○) while incubating with $[Cp^*Rh(bpy)(H_2O)]^{2+}$ (0.2 mM) in sodium formate (0.15 M) at 37°C.

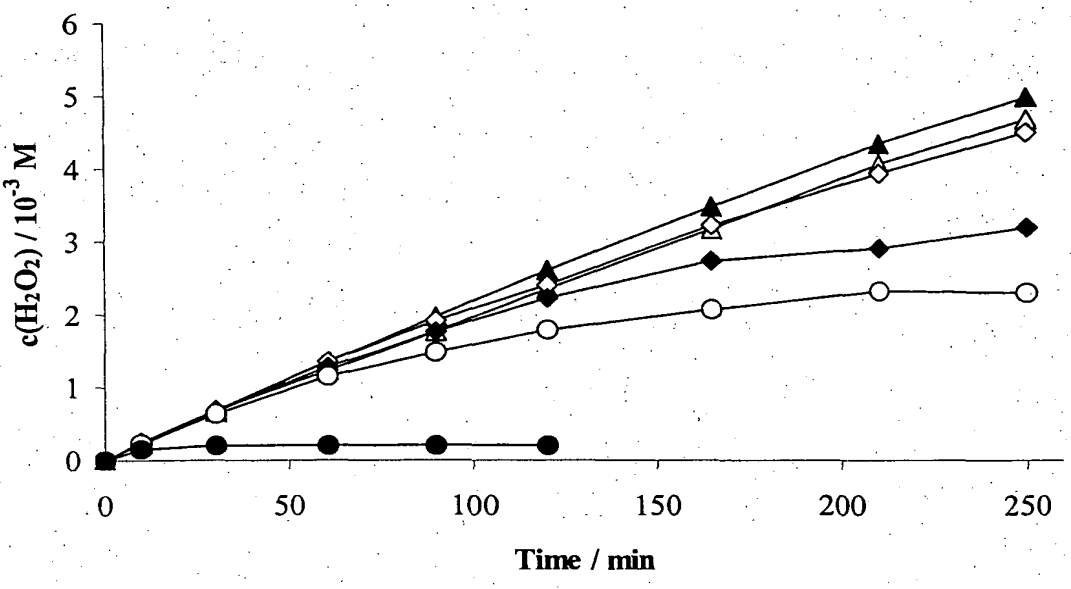

Figure 17: Time course of hydrogen peroxide formation at different ratios $[Cp^*Rh(bpy)(H_2O)]^{2+}$ / FAD. $c([Cp^*Rh(bpy)(H_2O)]^{2+})$ = 19 μM, $c(NaHCO_2)$ = 0.15 M, T = 37°C, c(FAD) = 0 μM (●) , 10 μM (○), 20 μM (◆), 50 μM (◇), 100 μM (▲), 200 μM (△).

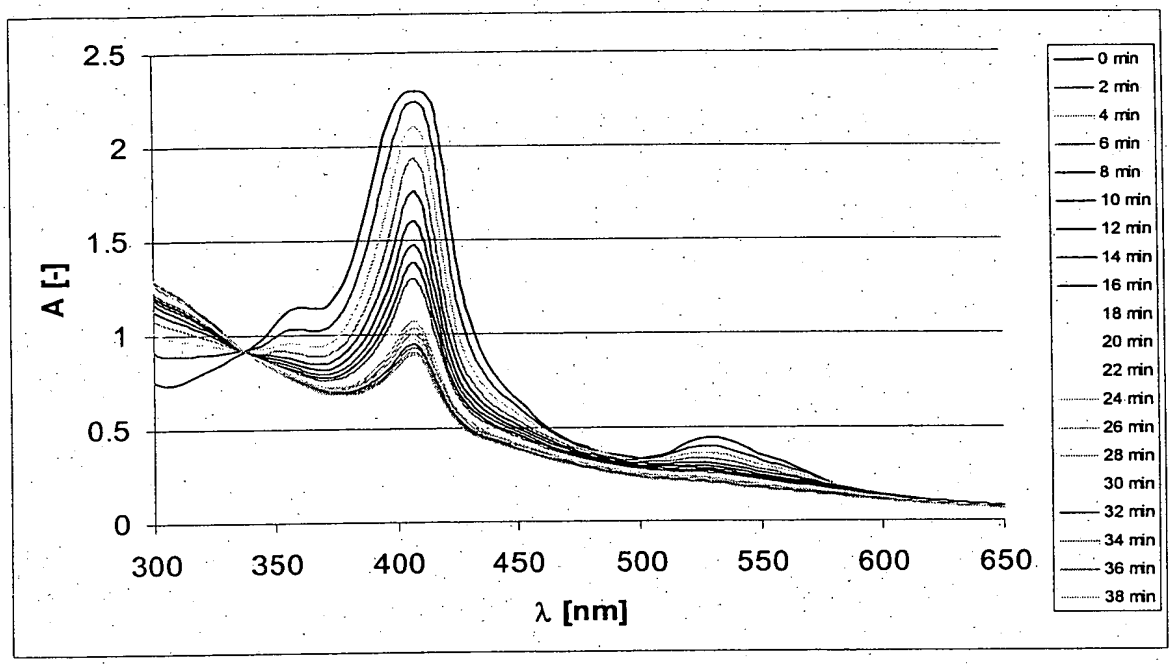

Figure 18: UV-spectra of a 50 μM Cyt C solution in the presence of 1 mM H_2O_2.

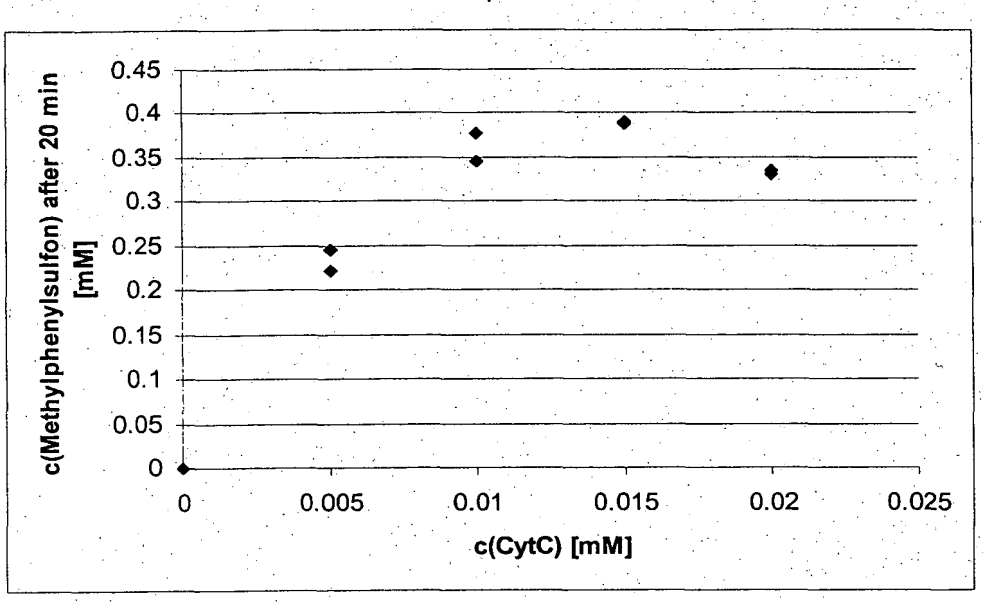

Figure 19: Dependence of the CytC-catalyzed sulfoxidation efficiency on c(CytC).

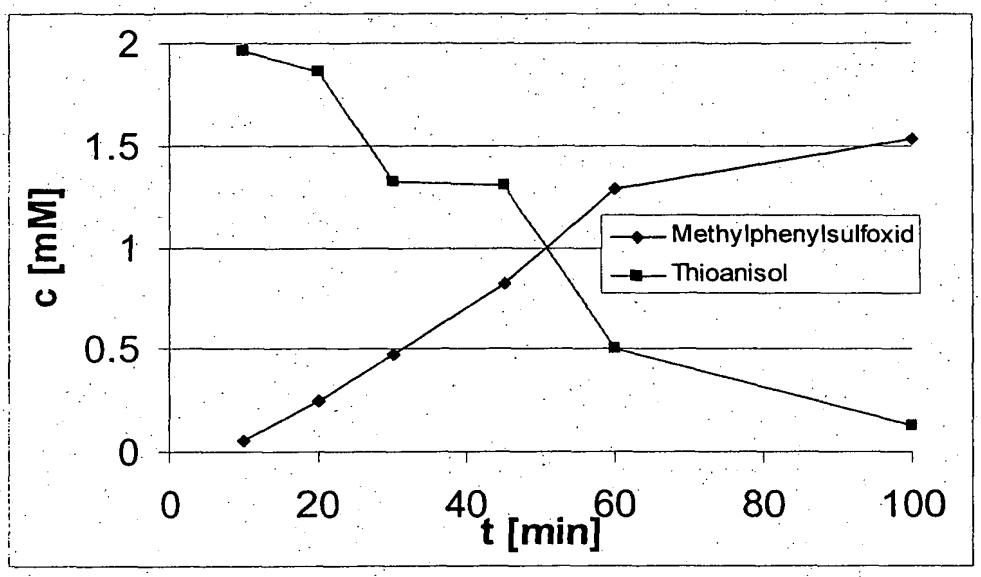

Figure 20: Time-course of CytC-catalyzed sulfoxidation of thioanisol with *in situ* generation of hydrogen peroxide by $[Cp^*Rh(bpy)(H_2O)]^{2+}$.

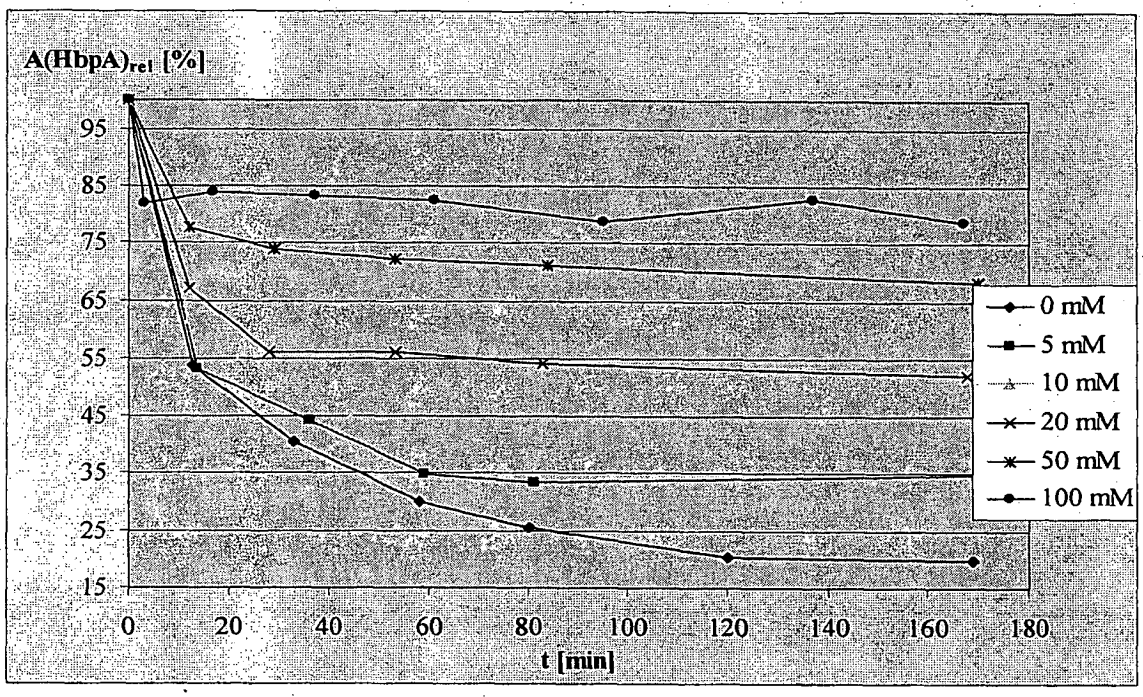

Figure 21: Residual HbpA activity while incubation with $[Cp^*Rh(bpy)(H_2O)]^{2+}$ and varying NH_3 concentrations.

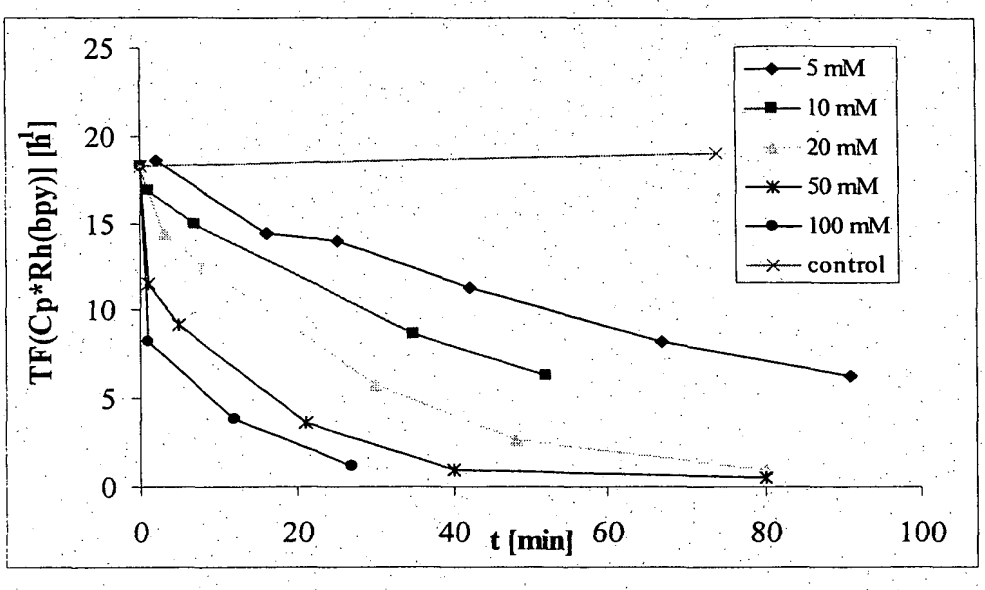

Figure 22: Inhibition of formate driven NADH regeneration catalyzed by $[Cp^*Rh(bpy)(H_2O)]^{2+}$ under varying NH_4^+ concentrations.

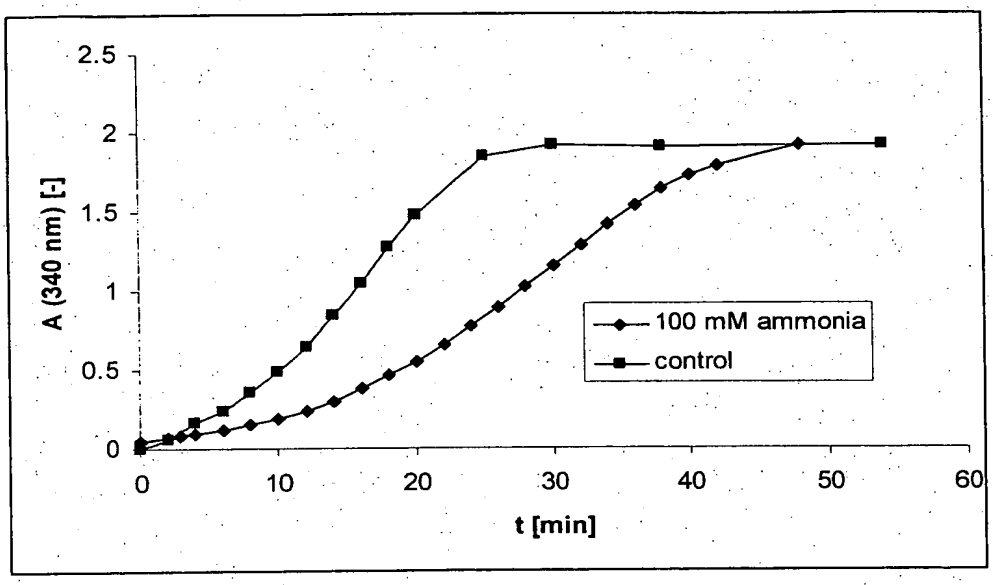

Figure 23: Feasibility of electrochemical NADH regeneration in NH_4^+ containing buffers.

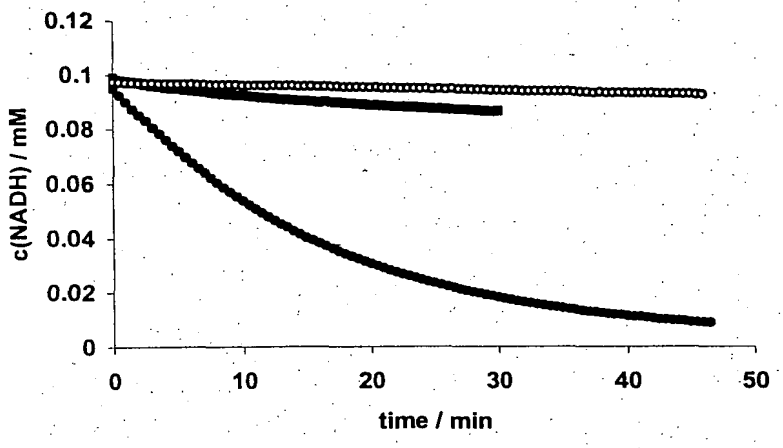

Figure 24: Oxidation of NADH by $[Cp^*Rh(bpy)(H_2O)]^{2+}$/FAD: $c(NADH)_0$ = 0.1 mM; T = 30°C; (■) only $[Cp^*Rh(bpy)(H_2O)]^{2+}$ (0.01 mM); (O) only FAD (0.04 mM); (●) both $[Cp^*Rh(bpy)(H_2O)]^{2+}$ (0.01 mM) and FAD (0.04 mM).

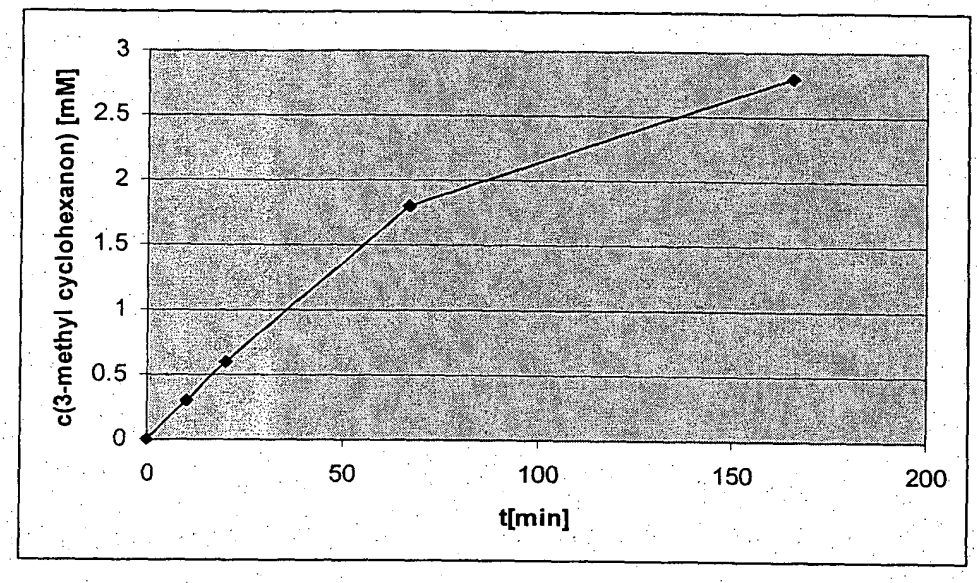

Figure 25: Time course of the oxidation of 3-methyl cylohexanol catalyzed by alcohol dehydrogenase from *Thermus sp.*. The necessary oxidized nicotinamide coenzyme was in situ generated from NADH.